Analysis of Microsegregation in Al-Si-Cu Ternary Alloys: Interdependence of Solute Composition at the Solubility Limit during Non-Equilibrium Solidification

Luis Antônio de Souza Baptista[a]* , *Késsia Gomes Paradela[a], Paulo Felipe Junior[a],*

Roberto Carlos Sales[a], Bruno Silva Dantas[a], Alexandre Furtado Ferreira[a]

[a]Universidade Federal Fluminense, Programa de Pós-Graduação em Engenharia Metalúrgica, Volta Redonda, RJ, Brasil

Virtually all metals used industrially undergo a solidification process during their production. Depending on the material and its manufacturing process, its physical/mechanical properties are affected to a greater or lesser extent by the microstructure and microsegregation obtained during the phase change. Aluminum casting alloys are good examples of products where this microstructure is vital for obtaining the desired properties. A sequence of experiments to analyze the upward vertical unidirectional solidification with transient heat transfer conditions in Al-Si-Cu ternary alloys was developed in the present work. The experimental results obtained were compared with classical microsegregation models. Discrepancies related to their use for ternary alloys were raised. Since the calculated results by these models do not take into account the influence of one alloying element on the solubility of the other element, disparities were founded between experimental and numerical results. A microsegregation model was proposed based on the solubility limits of the Si in the alloy as a function of the Cu concentration present in the liquid. The model, combined with the concepts of classical microsegregation theory, allows a realistic description of the microsegregation phenomenon. The model showed an excellent agreement between microsegregation profiles of solute experimentally measured and calculated.

Keywords: *Unidirectional solidification, Al-Si-Cu ternary alloys, dendritic structure, microsegregation, thermal parameters, modeling.*

1. Introduction

Aluminum has been commercially produced for about 150 years and in this short time, its industry has expanded and is present in the world's major poles. It is the most important of the non-ferrous metals and is among the most consumed currently. The rapid and remarkable growth of its use is due to its versatility and physical properties, especially its low density compared to other metals of great consumption, corrosion resistance, low melting point, and high electrical conductivity. These characteristics found in this material have motivated researchers to develop aluminum alloys in various systems and dozens of compositions. In this sense, the ternary Al-Cu-Si alloys, which have excellent fluidity, high mechanical strength, and low weight, stand out as an adequate choice as foundry alloys[1]. Another aspect is the intense demand from the automotive and aerospace industry, for products based on light alloys with higher specific strength and stiffness. The mechanisms that govern the transformation of liquids into solids are quite complex and their better understanding can improve metal design and production. Segregation phenomenon cannot be avoided during the solidification process since it is the consequence of the solubility difference between the liquid and the solid phases as well as of non-equilibrium solidification conditions.

The segregation has gotten the attention of researchers for many years[2-5]. However, the physical and chemical processes involved are highly complex and have always been an obstacle for modeling. To tackle the problem, it is common to concentrate the analysis in one of the two different spatial scales, i.e. macro or microsegregation. Some authors have a focus on the macrosegregation problem[5-7]. Although both processes are interconnected, the present work will be concentrated on the microsegregation scale. Most of the developments that occurred in the last decades were obtained by applying basic concepts and by systematic empirical work. The development of the microstructure and the segregation of solute during this phase transformation are controlled by phenomena occurring over a wide range of space and time scales. Studies have shown that the significant variables for solidification control are: solidification velocity (V_S), thermal gradient ahead of the solid/liquid interface (T_G), cooling rate (C_R) and concentration and redistribution of solute, which are interconnected through constitutional supercooling[8]. These variables can be correlated with the microstructure obtained with the use of metallography techniques. The complexity of the processes involved has, as a consequence, that a large majority of the studies presented in the literature[9-11] have been focused on binary alloys where physicochemical properties are more easily described, eliminating mutual interactions

*e-mail: lbaptista@id.uff.br

during the solidification process. The experimental works with ternary alloys[12,13], pointed out that a new approach has to be developed to allow the predicting of the microsegregation phenomenon, which should be taking into account the interaction of one alloying element on the solubility of the other during the solidification process. Several analytical models of microsegregation are found in the literature[14-26] describing the redistribution of the alloying elements during the solidification of the metals. In these models, the analytical treatment of microsegregation is based on the mass balance analysis of the solutes. The simplest formulation is the equilibrium model (lever rule) which describes the extreme case of the ideal balance between solid and liquid throughout the solidification process. The assumptions used for equilibrium solidification are difficult to obtain under actual industrial conditions. Brody and Flemings[17] proposed a mathematical model to include the back-diffusion effects. This solidification model assumes: 1) complete diffusion in the liquid phase and incomplete back-diffusion, 2) a plate-shaped dendrite geometry, 3) a constant diffusion coefficient, and 4) a linear or a parabolic solidification rate. Both equations derived by Brody and Flemings for linear and parabolic solidification rates are, however, invalid for rapid diffusion in the solid phase. Bower et al.[18]. and Clyne and Kurz[16] modified the Brody and Flemings equation for a parabolic solidification rate. This modification is valid for infinite and infinitesimal diffusion coefficients. Besides, the authors derived an exact solution for the Brody and Flemings solidification model for a parabolic solidification rate and showed that the accuracy of all the approximate solutions mentioned above is often poor. Although the Brody and Flemings solidification model with parabolic growth has been rigorously solved, several problems remain in applying the model to the solidification process: 1) calculating the exact solution is uncomfortable because the solution has an infinite series of the confluent hypergeometric functions, 2) no realistic method was found to estimate the solidification velocity or the local solidification time, a necessary value for the calculation, and 3) a parabolic solidification velocity in the assumptions may not be realistic in most solidification processes. In particular, the temperature at the solid-liquid interface and the solute redistribution during solidification must be taken into account to determine the rate of solidification. Depending on the solidification velocity several other models have been developed ranging from the back-diffusion model[18], the Scheil-Gulliver model[15] where there is no diffusion in the solid and complete homogenization in the liquid and models[26] that considers an even higher solidification velocity where the solute distribution in the liquid is controlled by diffusion. Modeling industrial casting processes, the Scheil-Gulliver model is more reasonable. The assumptions[15] of this model are negligible supercooling during solidification, total diffusion of the solute in the liquid and no diffusion into the solid. This model is different from the lever rule since it considers that there is no diffusion in the solid and, therefore, once solidified the solid composition no longer changes. On the other hand, there is a complete mixture in the liquid. The segregated solute from the solid phase increases the concentration of the liquid until it reaches the concentration of the eutectic. When a fast solidification process occurs, the velocity of the solidification front is

not low enough to allow the homogenization of the liquid and, therefore, a solute rich layer will be formed in the solidification front. The solute concentration will go through an initial transient and, then, a permanent regime will occur in which the rejection rate of the solute will be equal to the diffusion velocity from the solidification front[3,8]. It should be emphasized that, since the rejected solute is strongly dependent on the solidification velocity and the solute diffusion is affected by the concentration gradient, it is expected that solute concentration in the formed solid becomes a function of the solidification velocity[3,8]. Considering the range of solidification velocities observed in the experimental apparatus, more compatible with the industrial environment, modeling assumptions of solid homogenization or even of diffusion in the solid are not reasonable. Several studies have been developed to model the solidification process under these conditions. Burton et al.[26], proposed the inclusion of the solidification front displacement velocity for analytical microsegregation models, replacing in the Scheil equation the equilibrium coefficient k_{eq} by a k_{ef}, an effective partition coefficient given by Equation 1.

$$k_{ef} = \frac{k_{eq}}{k_{eq} + \left(1 - k_{eq}\right) exp^{(-V_s \delta / D)}} \tag{1}$$

Where V_S is the solidification velocity (m. s^{-1}), δ is the diffusion boundary layer thickness (m) and D is the diffusion coefficient of the solute in the liquid (m^2. s^{-1}). The value of diffusion boundary layer thickness (δ) depends on the solidification velocity, the viscosity of the liquid and the stirring conditions ahead the solid-liquid interface, and can vary approximately from 10^{-6} to 10^{-3} m[27]. It should be emphasized that in both models, Scheil and Burton, it is considered equilibrium in the solidification front and the solute concentration in both phases is related by k_{eq}. The limitation for applying the existing theoretical models in the present work is that they were developed for binary alloys and, consequently, do not consider the influence of one solute on the solubility of another. In other words, the models consider a constant k_{eq} value. Some authors have already discussed the need for better methodologies in determining the prior mentioned coefficient[28], but they are restricted for binary systems. By observing the ternary Al-Si-Cu diagram, in the isotherms shown in Figure 1, it can be seen that the solubility of Si in Al is affected by the presence of Cu. An increase in Cu concentration in the liquid reduces the solubility of Si in the solid.

2. Experimental Procedure

The experimental technique used in the present work was previously described in more detail[12,13,30]. Two ternary alloys (Al−9.0wt%Si−4.0wt%Cu and Al−9.0wt%Si−2.0wt%Cu) were prepared from high-purity materials (99.9% Al, 99.7% Si and 99.9% Cu) in a furnace at 800 ºC. The chemical compositions of the ternary alloys were confirmed by conventional spark emission spectroscopy. The melt was poured into a vertical upward unidirectional solidification apparatus, as shown in Figure 2. The bottom part of the steel mold was closed with a thin carbon steel sheet, which physically separates the melt from the cooling fluid. The initial melt temperature (M_T)
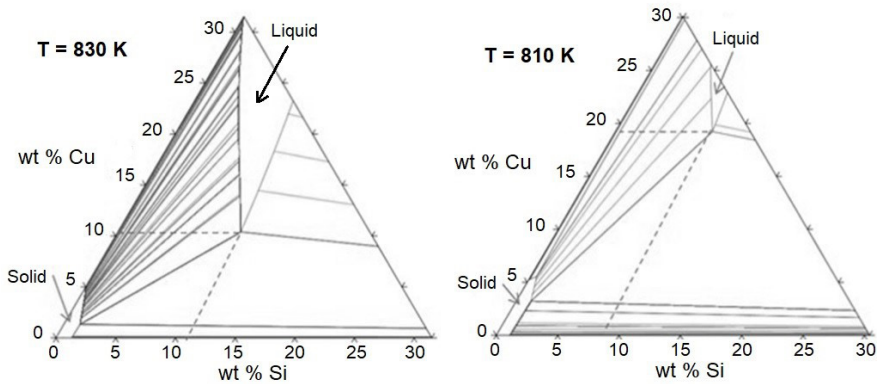
Figure 1. Ternary Al-Si-Cu diagram calculated by Thermo-Calc[29] software.
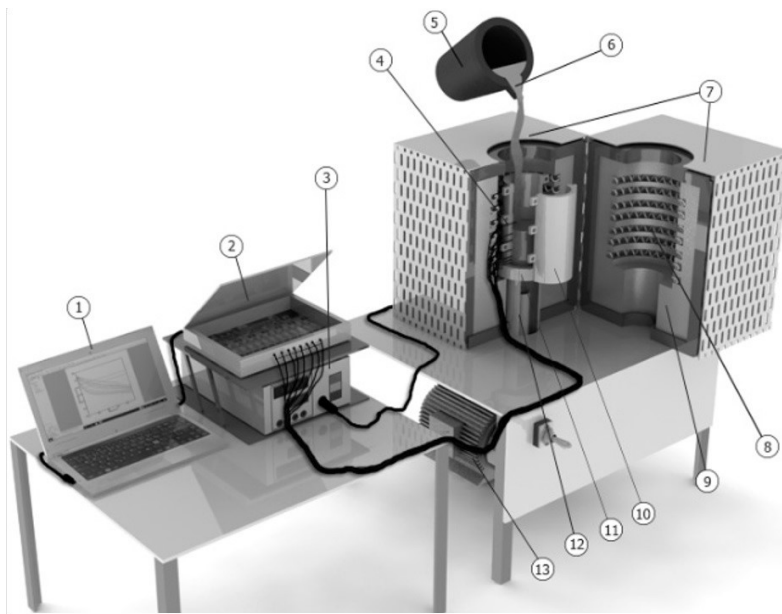
Figure 2. Diagrammatic representation of equipment: (1) personal computer and data acquisition software; (2) data logger hardware; (3) temperature controller system; (4) type K thermocouples; (5) crucible; (6) melt; (7) unidirectional solidification furnace; (8) electric heaters; (9) ceramic fiber insulation; (10) steel mold; (11) steel plate; (12) water-cooled system; (13) water pump.

was standardized at 55 °C above the liquidus temperature (L_T). The mold bottom was polished allowing a good contact condition at the metal/mold interface and, therefore, a higher overall metal/coolant heat transfer coefficient. Continuous temperature measurements in the castings were monitored during the solidification experiments. Eight thermocouples were positioned at 5, 10, 15, 20, 35, 45, 60 and 85 mm from the heat-extracting surface at the mold bottom. All of the thermocouples were connected to the data logger interfaced with a personal computer, and the temperature data were acquired automatically in a 100 Hz acquisition cycle. The cylindrical castings (145 mm height) were sectioned along its vertical axis, polished (500, 600, 800, 1000 e 1200 mesh sandpaper and 6 μm diamond paste) and etched with an acid solution 0.5%HF to reveal the micro−macro structure[31,32]. A JEOL scanning electron microscope (JEOL, Ltd., Japan) model JSM 6460LV with an Oxford energy-

dispersive spectrometer (Oxford Instruments), was used for the composition measurements. For microsegregation profiles measurements, the probe track initiates in the center of a dendrite arm and ends in the center of an adjacent arm, resulting in 100 measurement points. Microsegregation profiles were measured in all 16 samples obtained from the region close to the 8 thermocouples in each of the two castings. To obtain statistical significance, the micro-segregation profile of the Cu and Si was obtained for four positions in each sample and the measurement was repeated if the values were outside a range of two standard deviations.

3. Results and Discussion

The results obtained in the present work, are presented in three sections. First of all, experimental results are presented and discussed. In the following section, microsegregation
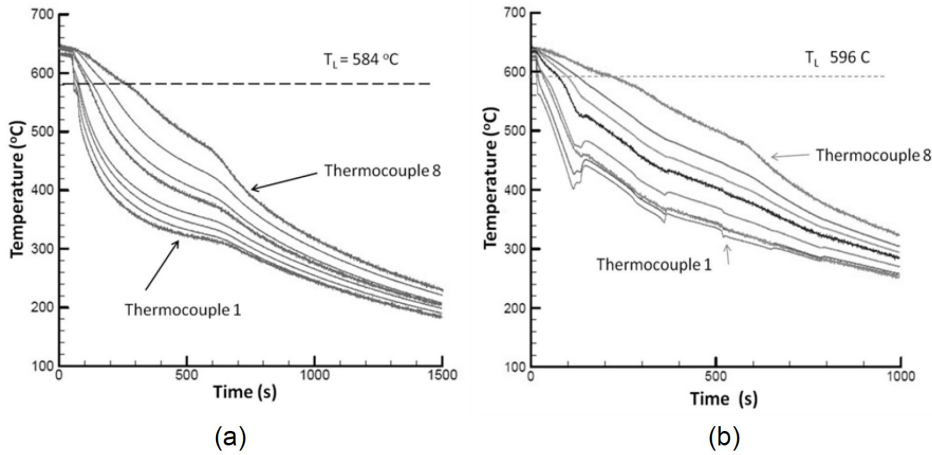
Figure 3. Experimental cooling curves obtained at different vertical positions (5, 10, 15, 20, 35, 45, 60 and 85 mm) from the heat-extracting surface of the casting: (a) ternary Al−9.0wt%Si−4.0wt%Cu alloy and, (b) ternary Al−9.0wt%Si−2.0wt%Cu alloy.

model based on the data obtained and its assumptions is proposed and, finally, model predictions versus experimental data are presented and discussed.

3.1 Experimental results

Figures 3a-b show the experimental cooling curves for the Al−9.0wt%Si−4.0wt%Cu alloy and Al−9.0wt%Si−2.0wt%Cu alloy castings. These cooling curves are similar to those presented by Sales et al.[30], one can see that temperature profiles decrease faster at positions closer to the mold bottom, and then gradually dwindles toward completion of local solidification. The water-cooled system used during the solidification experiments favors a higher solidification rate at the positions close to the mold bottom. Macrographic analysis of both casts has shown an aligned dendrite structure with the heat extraction direction.

Figure 4 shows the solidification velocity as a function of the distance from the chill for both castings.

Figure 4 also shows the magnitude difference that occurred in the solidification velocity values with the position along the casting length for the different copper content (2.0wt%Cu and 4.0wt%Cu). Analyzing the experimental tendencies in the graph of Figure 4, it can be inferred that the copper solute added in aluminum alloy, from 2.0wt%Cu to the 4.0wt%Cu, had an impact on the solidification velocity values. This means that lower solidification velocities are found when the copper solute concentration is increased in aluminum alloy. The slight deviation found between experimental curves is due to the increase in the copper content, which in turn caused a decrease in the liquidus temperature. The local concentration of the solutes (Si and Cu) in any position of the ingot is considered to be the alloy initial concentration. Macrosegregation is not considered during the calculations due to the adopted conditions in the experiments, i.e., segregation phenomenon is typical of Aluminum alloys with a high concentration of copper solute, in the present work a small concentration of copper was used during the solidification experiments, and, the casting conditions employed here are expected to reduce the macrosegregation severity during solidification (in this study the higher solidification speed observed was 1.5 mm/s at the 5 mm position, while works[7] focused on the
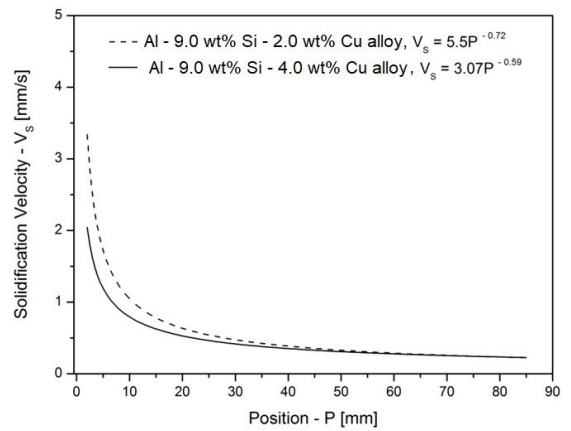
Figure 4. Solidification velocity (V_s) as a function of position (P) from the heat extraction surface: ternary Al−9.0wt%Si−4.0wt%Cu alloy and ternary Al−9.0wt%Si−2.0wt%Cu alloy.
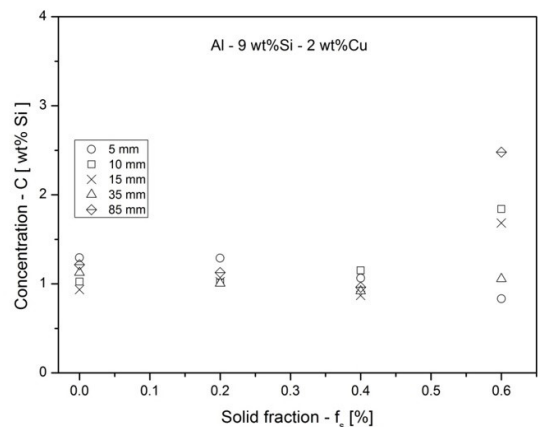
Figure 5. Si microsegregation of the Al-9.0wt%Si-2.0wt%Cu alloy.

macrosegregation use a much higher solidification speed). Figures 5 and 6 depict the observed microsegregation profiles for Si and Cu in Al−9.0%wtSi−2.0%wtCu alloy at positions of 5, 10, 15, 35 and 85 mm.

Analysis of Microsegregation in Al-Si-Cu Ternary Alloys: Interdependence of Solute Composition at the
Solubility Limit during Non-Equilibrium Solidification

5
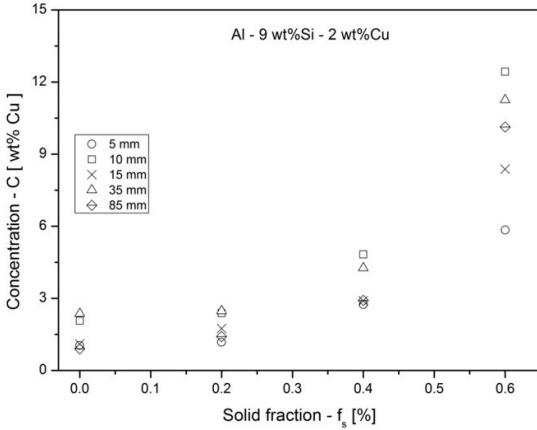
Figure 6. Cu microsegregation of the Al-9.0wt%Si-2.0wt%Cu alloy.
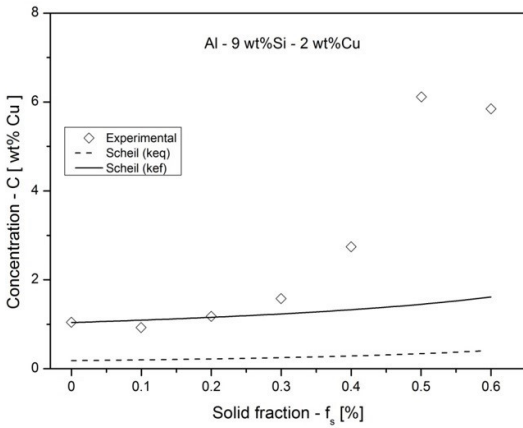
Figure 7. Cu microsegregation predicted by the Scheil equation using k_{eq} and k_{ef} for the 5 mm position for the ternary Al-9.0wt%Si-2.0wt%Cu alloy.

Table 1. Diffusion coefficient and diffusion boundary layer thickness.

Element	D_L (m^2.s^{-1})	δ (m)
Si	3.0×10^{-9}	5.0×10^{-6}
Cu	3.6×10^{-9}	1.0×10^{-5}

The concentration values of solute versus solidified fraction present the expected profiles, i.e. both concentrations of the solutes seem to increase gradually with the solidified fraction. On the other hand, the experimental data are not conclusive as to the solidification velocity effect on the concentration profiles. In previous studies presented by Paradela et al.[27] and Ferreira et al.[33], the concentration profiles move upward with the increase in solidification velocity. However, binary alloy systems were considered in those works presented by authors. In the binary Al-Si and Al-Cu alloys, the phase diagrams allow an estimation of the values of k_{eq} and maximum solubility[20,34]. In the case of ternary diagrams, the solubility of one element can be affected by the presence of the other[35]. In addition, the solidifying liquid may undergo concentration changes due to solute rejection at the solidification front ($k_{eq} < 1$) and this change in concentration is strongly affected by the solidification velocity. Consequently, solubility in the solid is difficult to estimate using traditional analytical models. It should be emphasized that since the employed alloys in this work, have an initial composition of 9% wt Si, already close to the eutectic composition, Si saturation in the liquid is rapidly attained so that the only independent variable in the process is the Cu concentration in the liquid. This causes the concentration of Si in the liquid to decrease during solidification with a consequent effect on the solute concentration of the formed solid. The Cu concentration experimentally obtained and calculated by the Scheil equation at the position of 5 mm, is shown in Figure 7. In that result, in order to improve the predictions of Scheil equation ($C_s = k_{ef}\, C_0\, (1 - f_s)^{\,KEF-1}$), the equilibrium partition coefficient (k_{eq}) is replaced by the effective partition coefficient (k_{ef}). Table 1 shows of the diffusion boundary layer thickness, δ (m), and is the diffusion coefficient of the solute in the liquid, D (m^2. s^{-1}) values used in the model[36,37].

It is interesting to highlight that two hypotheses were used: a) No diffusion in the solid and total mixing in the liquid is considered in the Scheil equation and; b) No diffusion in the solid and diffusion in the liquid region are adopted by the Burton method. The values of k_{eq} were obtained from the isotherms of the ternary Al-Si-Cu diagram generated by Thermo-Calc[29] software for the liquidus and solidus temperature of the alloy under study. The maximum equilibrium solubility of Cu in Al (FCC) obtained through the phase diagram generated by Thermo-Calc[29] for the ternary system is 5.15% wt Cu, with precipitation of other Cu rich phases. The Cu microsegregation data at the position of 5 mm are as expected by classical modeling, i.e. Cu concentration increases as the solid fraction goes up. The Scheil equation with k_{eq}, based on the hypothesis of total homogenization of the liquid, predicts a lower solute concentration than the experimentally observed. Under a high solidification velocity ($P = 5$ mm) a better match is observed using Scheil equation with k_{ef}. As previously discussed, the k_{ef} is determined from the Burton method, which considers solute accumulation in the solidification front and this, in turn, favors a higher solute concentration in the solid region. Taking into account the solidification velocity in the determination of k_{ef} as shown in Equation 1, the range of values for k_{ef} goes from k_{eq} (for V_S approaching zero) to 1 (for V_S approaching infinity). The values of Cu concentration calculated by Scheil equation with k_{ef} are directly affected by the V_S. The profile of Cu calculated by the Scheil equation, has the expected behavior for a binary system with no interaction between solutes, i.e. the profile of Cu moves upward with the increase in V_S. Figure 8 shows the Si concentration versus the solid fraction. The Si profiles were determined from the solidification experiment and calculated by the Scheil equation with k_{ef} and k_{eq}. The Si concentration obtained experimentally are lower than those predicted by the Scheil equation with k_{ef}, which indicates that other factors not foreseen in the initial hypotheses should be taken into account. Going back to Figure 1, it can be observed that Cu solubility in the liquid is about 25.6% wt Cu at the end of solidification, therefore, Cu segregated from the solid to the liquid during solidification can be absorbed by the remaining liquid.
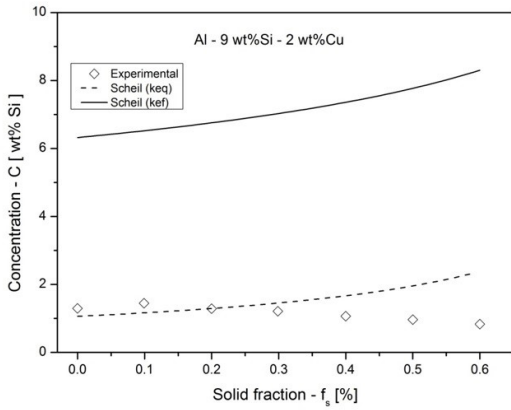
Figure 8. Si micro-segregation predicted by the Scheil equation using k_{eq} and k_{ef} for the 5 mm position for the ternary Al-9.0wt%Si-2.0wt%Cu alloy.
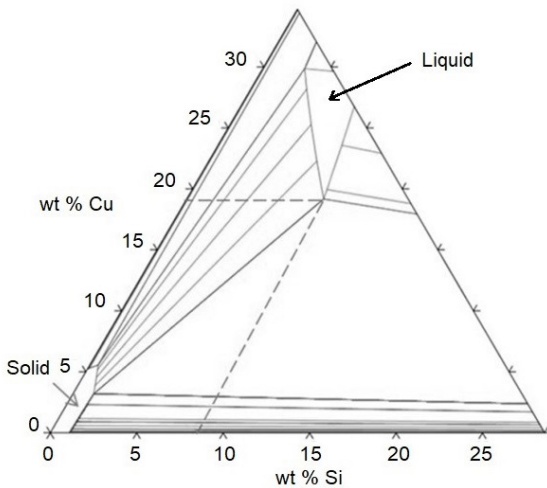
Figure 9. Al-Si-Cu system isotherm at 999 K.
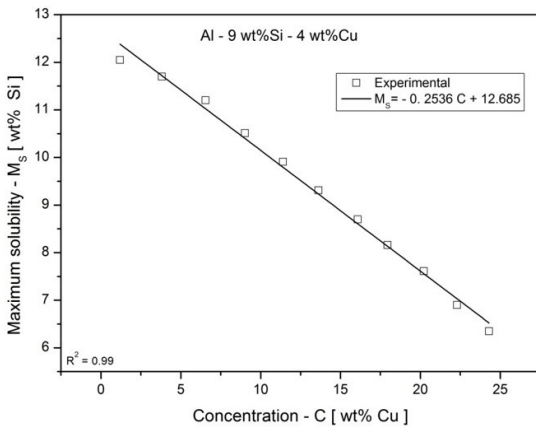
Figure 10. Maximum Si solubility in the liquid as a function of Cu concentration.

A more careful analysis of the ternary Al-Si-Cu diagrams (Figure 1) shows that the effect of increasing in Cu concentration in the liquid reduces the solubility limit of Si in the liquid phase and, consequently, limiting its content

in the FCC solid. Both the Scheil equation and the Burton method were developed for binary alloys and do not take into account the influence of one solute on another in the partition coefficient[14,26]. One of the assumptions of the models is the constant value of k_{eq} and the absence of solubility limits. During solidification processes under high solidification velocities, Cu is segregated into the solidification front and, therefore, the liquid close to the interface becomes rich in Cu. As one moves away from the solidification front, Cu concentration decreases almost exponentially, towards their initial value in the liquid. Returning to the isotherms of the Al-Si-Cu ternary phase diagram in the Figure 1, it is found that increasing the Cu concentration in the liquid causes the equilibrium Si concentration in the solid phase Al FCC to be drastically reduced. For example, a 4.0%wtCu and 9.0%wtSi liquid (one of the alloys used in the solidification experiments) would have a 1.12%wtSi solid in equilibrium. However if, due to the solute wave generated in the solidification front, the content of Cu goes to 20%wt in that liquid region, the maximum solubility of Si solute in the liquid drops to 7.9wt%Si, so that the solid in equilibrium has only 1% wt Si, as shown in Figure 9. In other words, the increase in Cu concentration in the liquid does not allow that Si concentration in the liquid region to rise and this, in turn, favors the lower Si concentration in the solid region.

This fact explains the low Si concentration experimentally observed in the region close to the water-cooled system, which has a high solidification velocity, as shown in Figure 8. Considering the premise of solute accumulation in the solidification front and solute diffusion in the liquid region; the solidification process with a higher velocity favors solute accumulation in that region. The Cu solute has a high solubility limit in the liquid it will be reasonable to consider that a higher solidification velocity will result in a higher Cu concentration in the solidifying liquid. The data obtained from Thermo-Calc[29] and presented in Figure 10 shows the maximum Si solubility in the liquid as a function of Cu content. These data show that an increase in Cu concentration decreases the maximum Si solubility in the liquid.

To facilitate the analysis, only the samples that are closer to the refrigerated base and, therefore, have higher solidification velocity are considered in Figure 11 (positions of 5, 10 and 15 mm). The Scheil equation predictions with k_{eq} are also plotted for comparison purposes. It can be seen that the predictions furnished by Scheil equation with k_{eq}, have significant deviations from the experimental data for the Al−9.0wt%Si−4.0wt%Cu alloy examined.

Both the Si concentration profiles obtained by the Scheil equation and experimentally increases gradually with the solidified fraction. However, experimental concentration profiles move downward for positions with higher solidification velocities. These experimental results suggest that, during solidification experiments, the Cu concentration at the solidification front increases resulting in a decreasing Si solubility in the liquid and, as a consequence, a decreasing Si content in the solidified material, i.e. a high Cu concentration in the liquid favors a reduction of Si content in the solidified region. To improve the prediction capability for the concentration profiles of Si solute, a microsegregation model based on the Si solubility

Analysis of Microsegregation in Al-Si-Cu Ternary Alloys: Interdependence of Solute Composition at the
Solubility Limit during Non-Equilibrium Solidification

7

limit in the solid region as a function of the Cu content in the liquid region is presented and discussed.

3.2 Microsegregation Model

A microsegregation model of ternary Al-Si-Cu system has been developed from following assumptions: 1) In the solidification front, the equilibrium between the phases is considered and, therefore, the solute concentration can be determined from the equilibrium partition coefficient ($C_L = C_S/k_{eq}$); 2) Cu have a high solubility limit since, even at the final stages of solidification, solute concentration higher than 20wt%Cu are possible to be achieved, in the liquid region. At fast solidification velocities, Cu concentration increase in the solidification front, which is controlled by diffusion, as discussed by Burton et al.[26]. The Cu concentration in the solid formed is calculated by the Scheil equation with

Figure 11. Si microsegregation for at the 5, 10 and 15 mm positions versus solidified fraction for ternary Al−9.0wt%Si−4.0wt%Cu alloy.

k_{ef}, which in turn, is determined via the Burton method, as a function of solidification velocity. Cu concentration in the liquid is estimated by assuming equilibrium at the solidification front. As the equilibrium partition coefficient, k_{eq}, is affected by the Cu concentration in the liquid, a better fit can be obtained by repeating the process iteratively until the difference between the values obtained is not significant; 3) The initial concentration of Si (9 wt%) is already close to the concentration of the binary Al−Si eutectic (12.48 wt% Si). The presence of the Cu solute moves the eutectic point to the left of the diagram, i.e. a higher Cu concentration in the liquid means a lower Si concentration at the eutectic point and, 4) At the beginning of the solidification the Cu concentration in the liquid is still not sufficient to bring the Si to its solubility limit, e.g., for the 9.0%wt Si in alloys used, the Cu concentration in the liquid would have to be 14.5%wt so that this value (9.0%wt Si) was the solubility limit of Si in the liquid. Therefore, the model is started assuming a microsegregation of Si following the model of Scheil. The Si concentration in the liquid is calculated considering premise (1), i. e., liquid-solid equilibrium at the solidification front and compares with the maximum Si allowed for the calculated Cu concentration in the liquid at the same position. If the Si concentration calculated using the Scheil equation is less than the maximum solubility calculated via Thermo-Calc software, Figure 10, the Scheil value is used, otherwise, the solubility limit value is considered. Figure 12 shows a simplified flowchart for the model.

This flowchart shows only a process view of the model since Cu equilibrium constant k_{eq} changes as a function of the Cu concentration in the liquid and all previous theoretical models are based on fixed values. To cope with this factor an iterative method was used. The model calculates the Cu concentration in the solid with an initial value for k_{eq} and from the new Cu concentration in liquid the process is repeated in
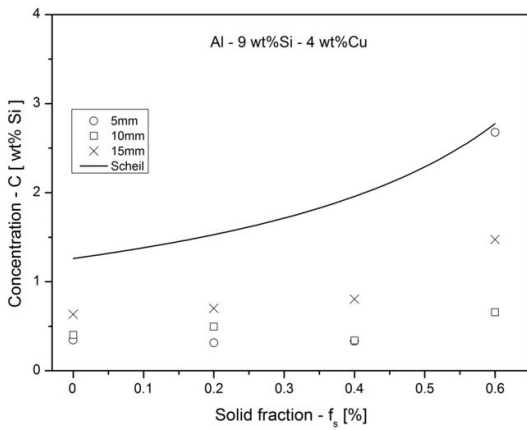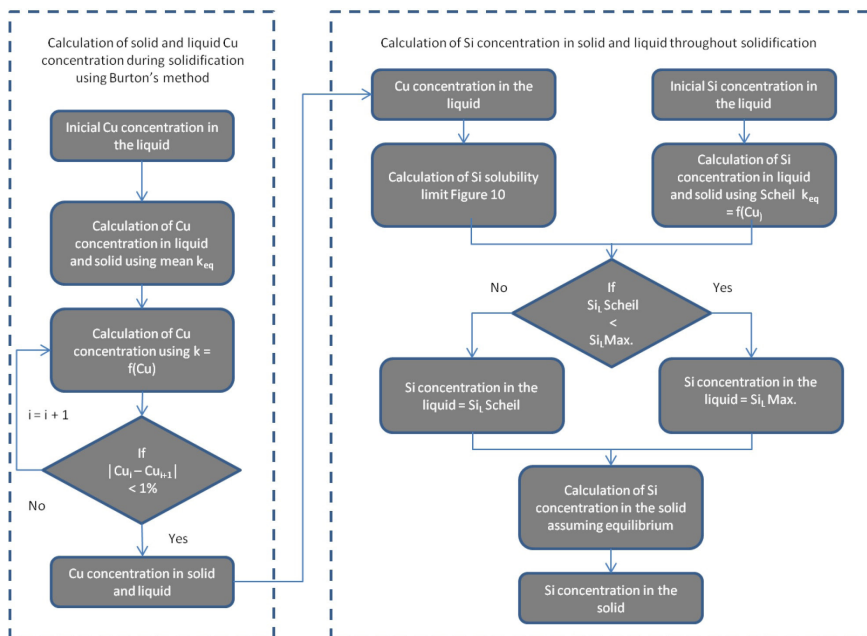
Figure 12. Simplified Model Flowchart.

order to obtain a new Cu concentration forecast. The cycle is repeated until the difference between the values is smaller than an acceptable value. The Si equilibrium constant and limit of solubility are them calculated as a function of the estimated Cu concentration in the liquid.

3.3 Model Forecasts versus Experimental Data

The model was initially compared to the experimental results obtained for the ternary Al−9.0%wtSi−4.0%wtCu alloy. Figure 13 shows the Si microsegregation profile at the position of 10 mm. The solid and dashed lines represent the proposed model in present work and Scheil equation with k_{eq}, respectively. To facilitate the comparison, the solid fraction was considered up to 0.8. Also included here is the prediction of the Scheil equation that emphasizes the peculiar behavior presented.

It is observed that the proposed model, which is obtained from the assumptions previously discussed, presents a better prediction when compared to the corresponding values for Si concentration calculated by the Scheil equation with k_{eq}. Figures 14 and 15 show respectively the concentrations of Cu and Si predicted by the model and experimental data for positions of 5, 10 and 15 mm. As expected, the Cu microsegregation profile, determined experimentally, moves upwards in regions close to the cooling plate, regions with higher solidification speeds.

A similar behavior is observed for Cu microsegregation calculated by the proposed model. Considering the Cu solute wave formation at the solidification front, a higher solidification velocity results in a higher solute content in that region and, consequently, higher Cu content in the solid region is found. Analyzing the experimental data in the graph of Figure 15, one can see an opposite behavior to the previously discussed in Figure 14, i.e. the values of Si concentration seem to decrease at regions close to the water-cooled system. Similar behavior also is observed for Si concentration calculated by the proposed model, the curves move downwards in the regions close to the cooling plate, where the higher solidification velocities were found. This is because the interaction between the Cu and Si solutes is considered in the proposed model, i.e. the presence of Cu solute limits the Si solubility in the liquid. Besides, the values of Si concentration calculated via model, show an excellent agreement with the experimental data.

When applying the proposed microsegregation model for the Al-9.0%Si-2.0%Cu alloy it is observed that the Cu content in the liquid at the beginning of the solidification is not sufficient to create a solubility limit for Si in the liquid. The values of Si concentration versus solid fraction at the position of 5 mm for ternary Al−9.0wt%Si−2.0wt%Cu alloy, are depicted in Figure 16, where the results calculated by the solubility limit model and the Scheil equation are plotted for comparison. The k_{eq} was considered in the Scheil equation in the prediction of the microsegregation profile. It was found that the Si concentration calculated by the Scheil equation is smaller than the maximum Si concentration possible for the Cu content calculated for this moment (solubility limit model). As the solidification proceeds, the Si and Cu concentrations increase. The Si concentration in the solidification front
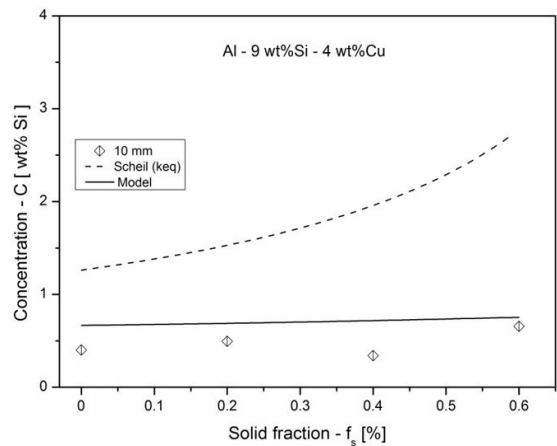
Figure 13. Si microsegregation versus solid fraction, at the 10 mm position.
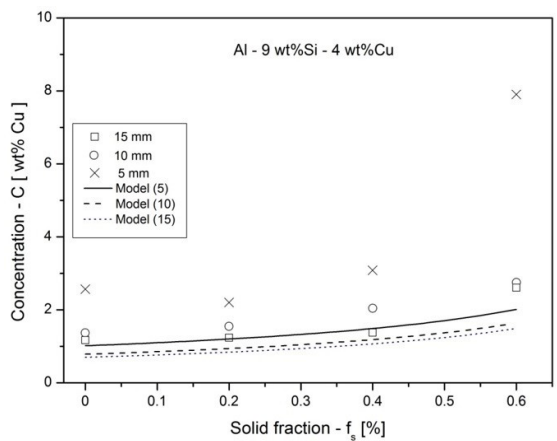
Figure 14. Cu microsegregation versus solid fraction, at the 5, 10 and 15 mm positions.
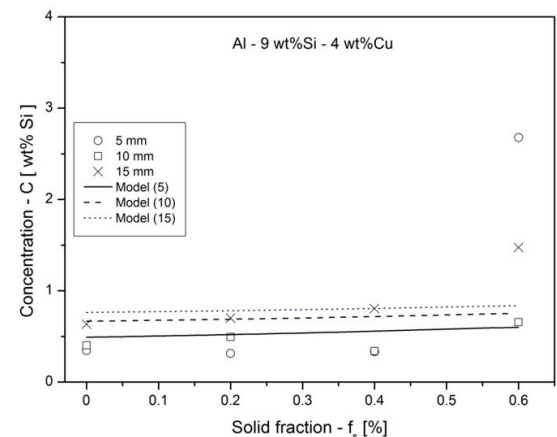
Figure 15. Si Microsegregation versus solid fraction, at the 5, 10 and 15 mm positions.

reaches the solubility limit created by the presence of Cu and the Si concentration becomes controlled by this limit.

Figure 17 shows the experimental microsegregation data for 5, 10 and 15 mm positions as well as the proposed model

Analysis of Microsegregation in Al-Si-Cu Ternary Alloys: Interdependence of Solute Composition at the
Solubility Limit during Non-Equilibrium Solidification

9
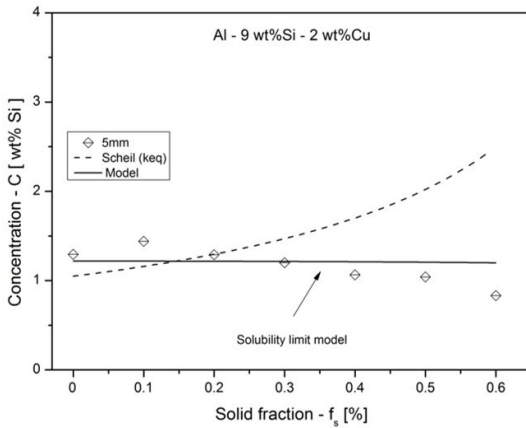
Figure 16. Si microsegregation versus solid fraction at the 5 mm position for Al-9.0wt%Si-2.0wt%Cu alloy.
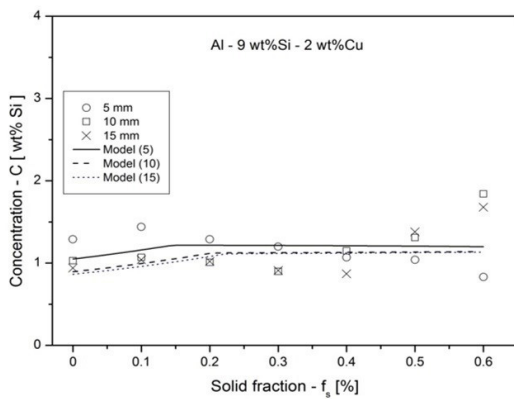
Figure 17. Si microsegregation versus solid fraction at the 5, 10 and 15 mm positions for Al-9.0wt%Si-2.0wt%Cu alloy. Experimental data x Proposed Model.

predictions for those positions. As can be observed the model correctly describes the Si microsegregation behavior, i.e., increasing concentration at the beginning of the solidification and them smoothly going down. It can also be observed that the Si concentration for the 5 mm position is higher than the others since at the beginning the Si concentration is still below the solubility limit and, therefore, the Si has the classical diffusion-controlled behavior. As the solidification proceeds, the Si concentration at the 5mm position becomes smaller than the concentration values observed at the other positions since the Cu concentration increases faster and, as a consequence, the solubility limit becomes smaller.

4. Conclusions

A unidirectional solidification study of ternary Al-Si-Cu alloys was performed. The solidification velocity during experiments was determined, and its effects on the microsegregation profiles were presented and discussed. The effect of the solidification velocity was incorporated into an effective partition coefficient and the Scheil equation was used in the prediction of the microsegregation profiles.

It was found that the Scheil equation has significant deviations from the microsegregation profiles experimentally obtained. Concerning the proposed model, good agreement between numerical results and experimental data is found. It is because the said model takes into account the interaction of one alloying element on the solubility of the other during the solidification process. The results pointed out that the presence of Cu solute creates a limit to Si solute solubility in the liquid region and consequently their concentrations in the solid region. On the other hand, in regions close to the water-cooled system and, therefore, with high solidification velocities, the profile of Cu microsegregation determined experimentally, move upwards with the solidification velocity. A similar behavior is found in the Cu microsegregation calculated by the proposed model. A higher solidification velocity results in the formation of a higher Cu solute wave at the liquid phase in the solidification front and, consequently, a higher Cu content in the solidified material.

5. References

1. Okayasu M, Takeuchi S, Ochi T. Mechanical properties of Al–Si–Cu Alloys produced by the continuous casting process with heating process. Int J Cast Met Res. 2017;30(4):217-25.

2. Canté MV, Spinelli JE, Ferreira IL, Cheung N, Garcia A. Microstructural development in Al-Ni alloys directionally solidified under unsteady-state conditions. Metall Mater Trans, A Phys Metall Mater Sci. 2008;39:1712-26.

3. Daloz D, Hecht U, Zollinger J, Combeau H, Hazotte A, Zaloznik M. Microsegregation, macrosegregation and related phase transformations in TiAl alloys. Intermetallics. 2011;19(6):749-56.

4. Ferreira AF, Paradela KG, Junior PF, Junior ZA, Garcia A. Phase-field simulation of microsegregation and dendritic growth during solidification of hypoeutectic Al-Cu alloys. Mater Res. 2017;20(2):423-9.

5. Ferreira IL, Garcia A, Nester B. On macrosegregation in ternary Al–Cu–Si alloys: numerical and experimental analysis. Scr Mater. 2004;50:407-11.

6. Ferreira IL, Santos CA, Voller VR, Garcia A. Analytical, numerical, and experimental analysis of inverse macrosegregation during upward unidirectional solidification of Al-Cu alloys. Metall Mater Trans, B, Process Metall Mater Proc Sci. 2004;(35):285-97.

7. Osório WR, Moutinho DJ, Leandro C, Peixoto LC, Ferreira IL, Garcia A. Macrosegregation and microstructure dendritic array affecting the electrochemical behavior of ternary Al–Cu–Si alloys. Electrochim Acta. 2011;(56):8412-21.

8. Khan MI, Mostafa AO, Aljarrah M, Essadiqi E, Medraj M. Influence of cooling rate on microsegregation behavior of magnesium alloys. J Mater. 2014;14:1-19.

9. Sigworth GK. Fundamentals of solidification in aluminum castings. Int J Met Cast. 2014;(8):7-20.

10. Dehnavi M, Vafaeenezhad H, Sabzevar MH. Investigation the solidification of Al-4.8 wt.%Cu alloy at different cooling rate by computer-aided cooling curve analysis. Metallurgical and Materials Engineering. 2014;20(2):107-17.

11. Goulart PR, Osório WR, Spinelli JE, Garcia A. Dendritic microstructure affecting mechanical properties and corrosion resistance of an Al-9 wt% Si alloy. Mater Manuf Process. 2006;22(3):328-32.

12. Baptista L A S, Ferreira AF, Paradela KG, Silva DM, Castro JA. Experimental investigation of ternary Al-Si-Cu alloy solidified with unsteady-state heat flow conditions. Mater Res. 2018;21(3):e20170565.

13. Baptista L A S, Paradela KG, Ferreira IL, Garcia A, Ferreira AF. Experimental study of the evolution of tertiary dendritic arms and micro-segregation in directionally solidified Al–Si–Cu alloys castings. Journal of Material Research and Technology. 2019;8(1):515-21.

14. Sarreal J, Abbaschian G. The effect of solidification rate on micro-segregation. Metall Mater Trans, A Phys Metall Mater Sci. 1986;17(11):2063-73.

15. Scheil E. Bemerkungen zur Schichtkristallbildung. Z Metallk. 1942;34:70-2.

16. Clyne T, Kurz W. Solute redistribution during solidification with rapid solid state diffusion. Metall Mater Trans, A Phys Metall Mater Sci. 1981;12(6):965-71.

17. Brody HD, Flemings MC. Solute redistribution in dendritic solidification. Trans Metall Soc AIME. 1966;236:615-24.

18. Bower T, Brody H, Flemings M. Measurements of solute redistribution in dendrite solidification. Trans Metall Soc AIME. 1966;236:624-33.

19. Ohnaka I. Mathematical analysis of solute redistribution during solidification with diffusion in solid phase. Transactions of the Iron and Steel Institute of Japan. 1986;26(12):1045-51.

20. Kobayashi S. A mathematical model for solute redistribution during dendritic solidification. Transactions of the Iron and Steel Institute of Japan. 1988;28(7):535-42.

21. Nastac L, Stefanescu DM. An analytical model for solute redistribution during solidification of planar, columnar, or equiaxed morphology. Metall Trans, A, Phys Metall Mater Sci. 1993;24(9):2107-18.

22. Rappaz M, Boettinger WJ. On dendritic solidification of multicomponent alloys with unequal liquid diffusion coefficients. Acta Mater. 1999;47:3205-19.

23. Easton M, Davidson C, St. John D. Effect of alloy composition on the dendrite arm spacing of multicomponent aluminum alloys. Metall Mater Trans, A Phys Metall Mater Sci. 2010;41:1528-38.

24. Voller VR. On a general back-diffusion parameter. J Cryst Growth. 2001;226(4):562-8.

25. Ferreira IL, Moreira ALS, Aviz J, Costa TA, Rocha O F L, Barros AS, et al. On an expression for the growth of secondary dendrite arm spacing during non-equilibrium solidification of multicomponent alloys: validation against ternary aluminum-based alloys. J Manuf Process. 2018;35:634-50.

26. Burton JA, Prim RC, Slichter WP. The distribution of solute in crystals grown from the melt. part i. theoretical. J Chem Phys. 1953;21:1987-91.

27. Paradela KG, Baptista L A S, Sales RC, Felipe P Jr, Ferreira AF. Investigation of thermal parameters effects on the microstructure, microhardness and microsegregation of Cu-Sn alloy directionally solidified under transient heat flow conditions. Mater Res. 2019;22(4). http://dx.doi.org/10.1590/1980-5373-mr-2019-0259.

28. Gharavol MHA, Sabzevar MH, Fredriksson H. Effect of partition coefficient on micro-segregation during solidification of aluminium alloys. Int J Miner Metall Mater. 2014;2(10):980-9.

29. Thermo-Calc Software AB [homepage on the Internet]. Sweden: Thermo-Calc Software AB; 2020 [cited 2020 Apr 28]. Available from: www.thermocalc.com

30. Sales RC, Felipe P Jr, Paradela KG, Garção WJL, Ferreira AF. Effect of solidification processing parameters and silicon content on the dendritic spacing and hardness in hypoeutectic Al-Si alloys. Mater Res. 2018;21(6):e20180333. http://dx.doi.org/10.1590/1980-5373-MR-2018-0333.

31. Abu-Dheir N, Khraisheh M, Saito K, Male A. Silicon morphology modification in the eutectic Al-Si alloy using mechanical mold vibration. Mater Sci Eng A. 2005;393(1-2):109-17.

32. Goulart PR, Spinelli JE, Osório WR, Garcia A. Mechanical properties as a function of microstructure and solidification thermal variables of Al-Si castings. Mater Sci Eng A. 2006;421(1-2):245-53.

33. Ferreira AF, Chrisóstimo WB, Sales RC, Garção WJL, Sousa NP. Effect of pouring temperature on microstructure and microsegregation of As-Cast aluminum alloy. Int J Adv Manuf Technol. 2019;104:957-65. http://dx.doi.org/10.1007/s00170-019-03979-6.

34. Martorano MA, Beckermann C, Gandin C-A. A solutal interaction mechanism for the columnar to-equiaxed transition in alloy solidification. Metall Mater Trans, A Phys Metall Mater Sci. 2003;(34):1657-74.

35. Medramo-Prieto HM, Garay-Reyes CG, Gomez-Esparza CD, Aguilar-Santillan JA, Maldonado-Orozeo MC, Martinez-Sanchez RM. Evolution of microstructure in Al-Si-Cu system modified with a transition element addition and its effect on hardness. Mater Res. 2016;19:1-7.

36. Qiang S, Yutuo Z, Haixia C, Chengzhi W. Phase field modeling of multiple dendrite growth of Al-Si binary alloy under isothermal solidification. China Foundry. 2008;5(4):265-7.

37. Wesner E, Chaoudhury A, August A, Berghoff M, Nestler B. A phase field study of large-scale dendrite fragmentation in Al-Cu. J Cryst Growth. 2012;359:107-21.